Application of CCHPs in a Centralized Domestic Heating, Cooling and Power Network – Thermodynamic and Economic Implications

Nami, Hossein; Anvari-Moghaddam, Amjad ; Arabkoohsar, Ahmad

Published in:
Sustainable Cities and Society

DOI (link to publication from Publisher):
https://doi.org/10.1016/j.scs.2020.102151

Publication date:
2020

Document Version
Accepted author manuscript, peer reviewed version

Application of CCHPs in a Centralized Domestic Heating, Cooling and Power Network – Thermodynamic and Economic Implications

Hossein Nami [a], Amjad Anvari-Moghaddam [b], Ahmad Arabkoohsar [b]

[a] Department of Mechanical Engineering, Faculty of Engineering, University of Maragheh, P.O. Box 83111-55181, Maragheh, Iran

[b] Department of Energy Technology, Aalborg University, Aalborg, Denmark

Abstract

The main objective of the present study is to utilize the waste heat and low-medium temperature geothermal heat sources in a centralized domestic heating, cooling and electricity network. Both geothermal and waste heat (from cement industry) are utilized to run domestic-scale combined cooling, heating and power (CCHP) units to meet the thermal and electrical demands of a residential area as the case study. Energy and exergy principles are applied to the designed CCHPs and the employed components, while exergoeconomic analysis is developed to show the economic feasibility of the proposed distributed energy systems. It is observed that the designed CCHPs not only meet the local energy demand in a sustainable way, but also deliver surplus thermal and electrical energy to the main grids. The thermodynamic analysis shows that under the base condition, the geothermal and waste heat driven CCHPs operate with sustainability index of 1.985 and 2.747, respectively. The economic evaluations demonstrated that, by using the proposed local CCHPs instead of the main grids to supply energy demand of the case study, it is possible to gain a benefit of 15687 € per year. This results in a lower energy payment of the end-users.

Keywords:

District heating and cooling; Centralized energy network; CCHP; Sustainability; Exergy

1. Introduction

Energy plays a key role in connection with the most important concerns of today and tomorrow like food security, sustainable development, climate change, health and environment protection [1]. Moving from traditional to smart energy systems (SESs) necessitates designing, analyzing, developing and utilizing transitional solutions to meet the required energy of human in different forms with enhanced performance for better sustainability [2]. In the meantime, secure supply of the dwellings' energy demand is a key element of SESs [3] where there must be a strong relation between district heating/cooling systems (DH/DC) and other energy sectors, especially electricity [4]. 40% of the overall energy usage and 36% of the emitted CO_2 in Europe are referred to buildings [5]. DH and DC systems are introduced as promising solutions to reduce energy consumption and emissions [6]. Different categories and the history of the technology development of these systems are described in detail in [7]. DH has a deeper history than DC, being introduced in the USA around 140 years back when steam was the main heat carrier through the pipes. Statistical surveys on the domestic heating and cooling systems show that, in Europe, around 6000 domestic heating networks are in operation delivering 11-12% of the total heat demand, while only 115 DC networks exist delivering 2% of the total cooling demand [5]. DC networks, especially those operated by renewables and waste heat resources, are highly recommended in terms of economy compared to the traditional cooling methods [8]. A wide variety of research works have been reported during the last years focusing on the feasibility of DH and DC networks. The following literature survey addresses some of the most recent publications in this area.

Todorov et al. [9] analyzed the integration of an aquifer thermal energy storage and ground-water heat pumps in DH and DC networks in terms of efficiency, techno-economic feasibility and impact on the surrounding groundwater resources. It was shown that combining DH and DC systems with seasonally reversible aquifer thermal energy storage has low impact on the aquifer area and is economically feasible. An index system was determined and visualized via a Geographic Information System (GIS) by Chen et al. [10] for ascertaining both temporal and spatial characteristics of district power loads caused by heating/cooling systems. It was also shown that operation modes and construction type could have great effects on the level and volatility of the district electric load caused by heating. Saberi et al. [11] investigated an improved system in a micro energy grid consisting of an energy hub system as a CCHP-based microgrid running with renewables like photovoltaic and wind. The main aim was to propose a multi-objective model that reduces carbon emission and operation cost in the presence of real-time demand response program. Oró et al. [12] considered waste heat harvesting from urban air cooled data centers to increase energy efficiency of DH networks. It was concluded that some cooling configurations, e.g. rear door cooling systems, are viable economically using waste heat recovery. Peltokorpi et al. [13] focused on defining the design frameworks of an organizational system for applying real-life applicable demand-side management innovations in DH and DC networks. The study revealed that in the organizational design it is needed to make a balance between the assignment of leadership and collaborative governance. Utilizing low-exergy sources for DH and DC networks for establishing sustainable dwellings was reviewed by Hepbasly [14]. Low-exergy systems are those heating or cooling systems that use low-valued energy flows delivered by sustainable energy sources, e.g. waste heat. He introduced different low-exergy heating and cooling systems and used low-exergy relations to estimate buildings' energy and exergy demands. It was observed that the exergy efficiency of utilizing low-exergy sources for DH and DC networks ranges from 0.4% to 25.3%, while it changes between 0.11% and 11.5% for greenhouses usage. Dorotić et al. [15] considered an energy system involving heating, cooling and power sections with the concept of future DH systems. Optimization of DH and DC networks with a multi-objective method and hourly timespan was carried out there. The objective functions of the optimization process were the environmental impacts (CO_2 emission) and the total system cost. The fact that large capital investment cost may limit the implementation of DH and DC networks was claimed by Sommer et al. [16]. Their idea for addressing this problem was to reduce the piping cost via system pressure reduction based on changing the connection of the expansion vessel. Development of a software tool to analyze the feasibility of the 5th generation DH and DC networks in both new and existing districts was published by Rhein et al. [17]. They considered all potential network designs for supplying their demands through the 5th generation DH and DC systems with renewables and waste energy flows as their main energy sources. The obtained results quantified the performance of the 5th generation DH and DC network based on numerous output metrics, including primary energy utilization, CO_2 emissions and network operation cost. Practical and economic benchmarking of sustainable cooling and heating supply options in southern European municipalities was done by Popovski et al. [18]. They concluded that the most competitive solution from a socio-economic point of view is to utilize the excess heat flows of industries. Thermodynamic, economic and environmental assessments of using waste gasification in a polygeneration system were reported by Kabalina et al. [19]. The aim was to supply domestic heating and cooling. It was shown that with a decrease in heating, cooling and electricity loads, the system could supply the demand using refuse-derived fuel or municipal solid waste as the main fuel. Carotenuto et al. [20] investigated low-temperature domestic heating and cooling systems driven by renewable energy sources. The combination of biomass, solar, and geothermal energy sources was considered for Monterusciello, a special location in Italy, as the case study. Although the primary energy ratio of 75% was obtained for the examined system, a long payback period (more than 20 years) showed that the plan was not economically feasible.

On the other hand, ORC is a mature technology and can be employed as a power generating system for a wide range of source temperatures [21]. In a recent research, Altun and Kilic [22] presented a thermodynamic evaluation of an operating geothermal driven 3 MWe ORC power plant. The thermodynamic assessment of the system was conducted to evaluate the energy and exergy efficiencies of each component, and the whole plant. Results revealed that the net power output might drop by 36% from winter to summer. In addition, from nighttime and daytime, the net power production may decrease by 5%.

In this study, two small-scale CCHPs fueled by geothermal and waste heat are considered in the present study as distributed energy systems. Both CCHPs are also equipped with ORC, single effect LiBr-H_2O absorption chiller and auxiliary heat exchangers to supply electricity, cooling (via chilled water) and heating (both space heating –SPH, and 80 °C for domestic hot water-DHW), respectively. A small residential area in Gaziantep, Turkey was considered as the case study. Since it was almost impossible to have access to high-resolution energy demand profile of the residents at the examined location, it is decided to calculate these profiles. Thermodynamic principles are applied at both component level and system level. In addition, for more reliable results, the economic benefits of using these local energy systems instead of the existing grids are taken into account in terms of household' payment. As the presented literature showed, the sustainable implementation of both supply- and demand-side management for DH and DC networks is often limited because of the existing complexity and the requirements to involve stakeholders. To the best of authors' knowledge, there is no study considering geothermal and industrial waste heat as the local available energy sources to provide energy demand (both thermal and electrical) of a specific neighborhood.

2. Network description

Fig. 1 indicates the connection of the residential area to the case study DH and DC network, in which energy demands are supplied via CCHPs. Considered topology is in such a way that all buildings have a separate access to the electricity, heating and cooling lines. The considered DH and DC network includes two small-scale CCHP units running via geothermal and waste heat sources and a dwelling network. Figs. 2 and 3 illustrate the geothermal and waste heat driven CCHPs, respectively.

A base-load condition is considered for each CCHP. It is also assumed that, under the base condition, half of the geothermal fluid (state 1 in Fig. 2 for the geothermal-driven CCHP) and half of the ORC exiting heat source (state 2 in Fig. 3 for the waste heat-driven CCHP) are fed to run the chiller. For the case of heating delivery, it should be mentioned that the presented system is a combination of the 3rd and the 4th generations of DH systems with the regular operating temperature of around 40 °C for SPH and 80 °C for DHW. It is supposed that the CCHPs will meet the heating, cooling and electricity demand of the considered residential area. Here, it is supposed that the considered neighborhood has an access to the main networks of power, cooling and heating. Therefore, if the peak energy demand exceeds the supplied value by the utilized CCHPs, then the extra energy will be compensated by the mains and vice versa. To obtain the energy demand profiles, required databases should be available. Since there is no access to these databases, the alternative solution is to estimate energy demand profiles. Therefore, some information according to the energy and comfort principles of the considered network, i.e. solar energy availability, buildings characteristics, information associated with the ambient condition, etc. are required. In the considered case study, it is supposed that the neighborhood contains 100 single-family separate houses, which will be covered by DH and DC systems. The main characteristics considered for the buildings as well as the environmental conditions are outlined in Table 1.

Table 1

Characteristics of the buildings as well as the environmental conditions [3,23]

Parameter	Value
Number of buildings with 1 / 2 / 3 / 4 / ≥ 5 residents	20 / 20 / 20 / 20 / 20
Living area of each building	150 (m^2)
Buildings shape	rectangular field of 15m × 10m
Comfort indoor temperature for SPH	20 - 24 °C
Comfort indoor temperature for space cooling (SPC)	24 - 27 °C
Windows area per building shell surface	20%
Walls surface per building shell surface	30%
Roofs area per building shell surface	25%
Floor area (including cold bridges) per building shell surface	25%
Average overall heat loss factor	0.93 $W/m^2.K$

Needed air exchange rate for ventilation	0.65 m^3/h per m^3
Effects of inhabitants' metabolism on the average daily internal heat gain of the building	2.3 °C

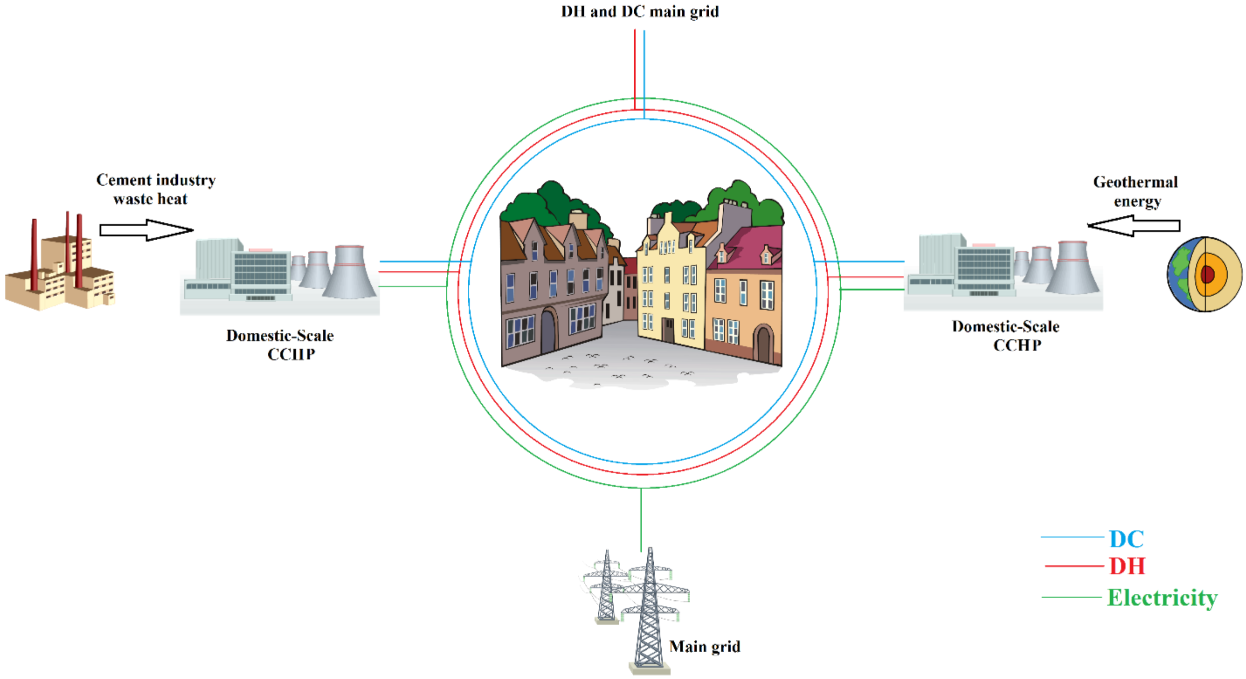

Fig. 1 Main layout proposed in the present study

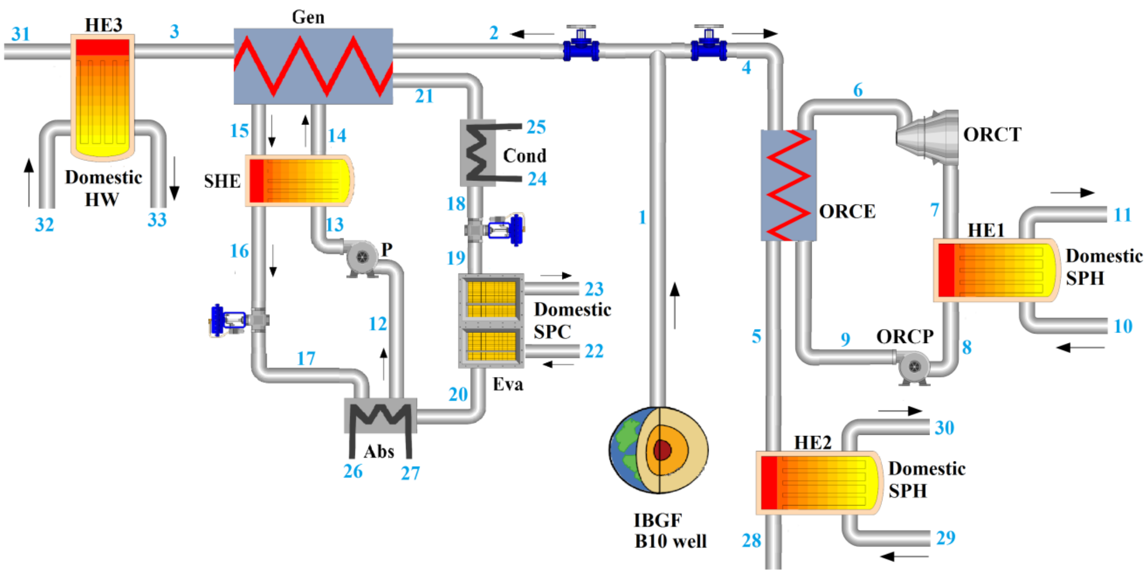

Fig. 2 Schematic diagram of the geothermal-driven CCHP

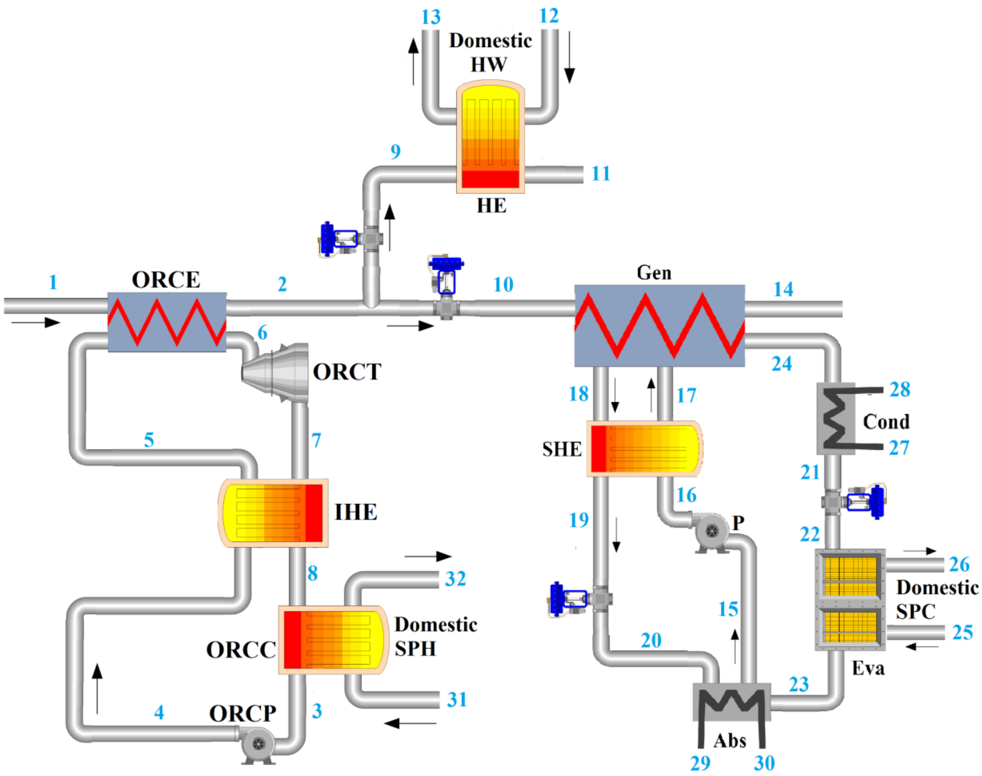

Fig. 3 Schematic diagram of the waste heat-driven CCHP

It should be noticed that the connection of the DH system to the building is based on the regular Instantaneous Heat Exchange Unit [23]. Fig. 4 illustrates the configuration of this substation. As the figure shows, there are two heat exchangers here, one is for hot water preparation and the other one is for space heating.

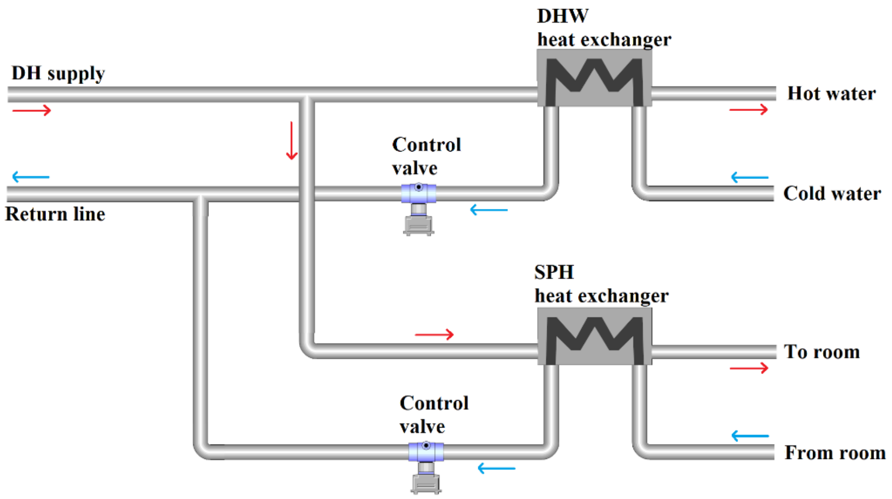

Fig. 4 An instantaneous heat exchange unit.

3. DH and DC systems mathematical modeling and main assumptions

Thermodynamic analysis of the presented DH and DC systems is divided into different subsections to give the possibility of describing each section in details. Different subsections are presented hereunder.

3.1.Geothermal driven small-scale CCHP

As presented in Fig. 2, geothermal driven CCHP is the combination of small-scale ORC, single effect absorption chiller and different heat exchangers to deliver DH. It should also be highlighted that the heat rejection within the ORC condenser is harvested to be used as SPH. Part of the geothermal source runs the ORC, while the rest is used to derive the chiller and after that provide DHW. Designing in this manner provides the flexibility of changing cooling supply and will adopt the system for different seasons. Pressurized water is used as the heat transfer fluid for delivering DHW, SPH and SPC. Main input data used in the geothermal-driven CCHP is listed in Table 2. The use of R123 is expected to be banned by the Montreal protocol. However, this usage-ban has not been applied yet and for the time being, not only that is used in a wide spectrum of research and practical works, but also it is well-proved that this refrigerant performs better than other commercially available refrigerants [21,24–27].

Table 2

List of input data utilized in the geothermal-driven CCHP modeling

Input data	Value	Unit
Geothermal volumetric flow rate [28]	70-80	m^3/h

Geothermal source temperature [28]	95-105	°C
Turbine and Pumps isentropic efficiency [29]	90 and 75	%
Temperature of coolant water [30]	20	°C
Temperature of DHW supply / return [31]	80 / 40	°C
Temperature of SPH supply / return [32]	35 / 20	°C
Temperature of SPC supply / return [33,34]	5 / 12	°C
Generator temperature	348 - 358	K
Heat exchangers effectiveness	85	%
Minimum allowed pinch temperature difference in ORCE	5	K
Average ambient temperature	298	K
Minimum allowed pinch temperature difference in Eva and Cond	5	K
ORC working fluid [29]	R123	-
ORCE pressure	250 - 400	kPa

In order to assess the geothermal-driven CCHP, thermodynamically, each component is considered as a control volume. Then, energy conservation and mass balance equation are applied as follows [35]:

$$\sum \dot{m}_i h_i + \dot{Q} = \sum \dot{m}_o h_o + \dot{W} \tag{1}$$

$$\sum \dot{m}_i = \sum \dot{m}_o \tag{2}$$

Table 3 outlines applied energy conservation equations for the proposed geothermal-driven CCHP components.

Table 3

Energy equations adopted for each component employed in the geothermal-driven CCHP [36]

Component	**Equation**	
ORCT	$\dot{W}_{ORCT} = \dot{m}_6 (h_6 - h_7)\,,\ \eta_{is,ORCT} = \dfrac{\dot{W}_{ORCT}}{\dot{W}_{is,ORCT}}$	(3)
ORCE	$\dot{m}_4 (h_4 - h_5) = \dot{m}_9 (h_6 - h_9)$	(4)
ORCP	$\dot{W}_{ORCP} = \dot{m}_8 (h_9 - h_8)\,,\ \eta_{is,ORCP} = \dfrac{\dot{W}_{is,ORCP}}{\dot{W}_{ORCP}}$	(5)
HE1	$\dot{m}_{10} (h_{11} - h_{10}) = \dot{m}_7 (h_7 - h_8)\,,\ eff_{HE1} = \dfrac{Max\{(T_7 - T_8),(T_{11} - T_{10})\}}{T_7 - T_{10}}$	(6)
HE2	$\dot{m}_5 (h_5 - h_{28}) = \dot{m}_{29} (h_{30} - h_{29})\,,\ eff_{HE2} = \dfrac{Max\{(T_5 - T_{28}),(T_{30} - T_{29})\}}{T_5 - T_{29}}$	(7)

HE3	$\dot{m}_3(h_3-h_{31})=\dot{m}_{32}(h_{33}-h_{32})$, $eff_{HE3}=\dfrac{Max\{(T_3-T_{31}),(T_{33}-T_{32})\}}{T_3-T_{32}}$	(8)
SHE	$\dot{m}_{15}(h_{15}-h_{16})=\dot{m}_{13}(h_{14}-h_{13})$, $eff_{SHE}=\dfrac{Max\{(T_{15}-T_{16}),(T_{14}-T_{13})\}}{T_{15}-T_{13}}$	(9)
Gen	$\dot{m}_2h_2+\dot{m}_{14}h_{14}=\dot{m}_3h_3+\dot{m}_{15}h_{15}+\dot{m}_{21}h_{21}$	(10)
Cond	$\dot{m}_{21}(h_{21}-h_{18})=\dot{m}_{24}(h_{25}-h_{24})$	(11)
Eva	$\dot{m}_{21}(h_{21}-h_{18})=\dot{m}_{24}(h_{25}-h_{24})$	(12)
Abs	$\dot{m}_{20}(h_{20}-h_{19})=\dot{m}_{22}(h_{22}-h_{23})$	(13)
P	$\dot{W}_P=\dot{m}_{12}(h_{13}-h_{12})$, $\eta_{is,P}=\dfrac{\dot{W}_{is,P}}{\dot{W}_P}$	(14)

3.2. Waste heat-driven small-scale CCHP

Waste heat-driven CCHP is shown in Fig. 3 and as can be seen it involves a recuperative ORC, a single effect absorption chiller and a heat exchanger to supply DHW. In the chiller unit, LiBr (lithium bromide) and water are considered as the absorbent and refrigerant, respectively. Waste heat source of the cement plant with specified characteristics was selected as the source. Table 4 lists the source condition. Since the considered waste heat source has a relatively higher temperature, MM as a known siloxane is considered as the working fluid and as a result recuperative ORC is employed instead of simple ORC [29]. Assumptions made for the CCHP modeling are the same as those presented in Table 2. In order to model the presented CCHP in Fig. 3 thermodynamically, all the employed components are supposed to be operated as a separate control volume and then energy conservation equations are adopted. Table 5 outlines these equations.

Table 4

Waste heat source properties [37]

Parameter	Temperature (°C)	Mass flow rate (kg/s)	Compositions
Value	250	18.43	0.689 N_2, 0.225 CO_2, 0.058 H_2O, 0.011 O_2, 0.01 Ar, 0.007 SO_2

Table 5

List of energy equations adopted for the components employed in the waste heat-driven CCHP [38]

Component	**Equation**	
ORCE	$\dot{m}_1(h_1-h_2)=\dot{m}_5(h_6-h_5)$	(15)

ORCT	$\dot{W}_{ORCT} = \dot{m}_6(h_6 - h_7)$, $\eta_{is,ORCT} = \dfrac{\dot{W}_{ORCT}}{\dot{W}_{is,ORCT}}$	(16)
IHE	$\dot{m}_7(h_7 - h_8) = \dot{m}_4(h_5 - h_4)$	(17)
ORCC	$\dot{m}_8(h_8 - h_3) = \dot{m}_{31}(h_{32} - h_{31})$	(18)
ORCP	$\dot{W}_{ORCP} = \dot{m}_3(h_4 - h_3)$, $\eta_{is,ORCP} = \dfrac{\dot{W}_{is,ORCP}}{\dot{W}_{ORCP}}$	(19)
HE	$\dot{m}_9(h_9 - h_{11}) = \dot{m}_{12}(h_{13} - h_{12})$, $eff_{HE} = \dfrac{Max\{(T_{13} - T_{12}),(T_9 - T_{11})\}}{T_9 - T_{12}}$	(20)
Gen	$\dot{m}_{10}h_{10} + \dot{m}_{17}h_{17} = \dot{m}_{14}h_{14} + \dot{m}_{18}h_{18} + \dot{m}_{24}h_{24}$	(21)
SHE	$\dot{m}_{16}(h_{17} - h_{16}) = \dot{m}_{18}(h_{18} - h_{19})$, $eff_{SHE} = \dfrac{Max\{(T_{17} - T_{16}),(T_{18} - T_{19})\}}{T_{18} - T_{16}}$	(22)
Cond	$\dot{m}_{24}(h_{24} - h_{21}) = \dot{m}_{27}(h_{28} - h_{27})$	(23)
Eva	$\dot{m}_{22}(h_{23} - h_{22}) = \dot{m}_{25}(h_{25} - h_{26})$	(24)
Abs	$\dot{m}_{20}h_{20} + \dot{m}_{23}h_{23} + \dot{m}_{29}h_{29} = \dot{m}_{30}h_{30} + \dot{m}_{15}h_{15}$	(25)
P	$\dot{W}_P = \dot{m}_{15}(h_{16} - h_{15})$, $\eta_{is,P} = \dfrac{\dot{W}_{is,P}}{\dot{W}_P}$	(26)

3.3.Residential area energy demand calculation

Thermodynamic model of the energy network (including DH and DC and electricity networks) is presented in this section. For doing the analysis, one needs to have a database of the loads in each sector. As there is no access to real users' energy consumption data due to privacy reasons, the energy consumption profiles (heat, cold and electricity) are estimated according to the number of residents, buildings' characteristics and standard patterns.

For the DH network, the total demand is the summation of DHW and SPH demands. In order to make a DHW consumption pattern, the randomly obtained profile of a normal single-family house without bathtub, given in Table 6, is used [3]. In order for making a reasonable simultaneity factor of the draw-off for the whole network, the given draw-off profile is randomized. With the aim of making the load profile compatible with a real case, the randomization in carried out in such a way that the distribution of the draw-offs for the periods “6:00-11:59 o'clock” and “18:00-23:59 o'clock” are at least three times larger than other periods of the day.

Table 6

Draw-off profile of a normal single-family dwelling/apartment without bathtub [3]

Time	Volume (lit)	Temperature (°C)	Duration (min)
10:55	43	40	5
10:55	15	45	2.5
11:05	0	0	0
11:15	42	40	5
11:15	15	45	2.5
11:25	0	0	0
11:35	42	40	5
11:45	0	0	0
11:55	42	40	5
// // // //	// // // //	// // // //	// // // //
22:55	42	40	5
22:55	15	45	2.5
23:05	0	0	0
23:15	42	40	5
23:15	15	45	2.5
23:25	0	0	0
23:35	42	40	5
23:45	0	0	0
23:55	42	40	5

On the other hand, several factors, such as the ambient and comfort temperatures and the building stuck characteristics could affect the energy demand for SPH. Considering all heat transfer terms between the building and the environment, energy demand in each building for SPH can be written as [39,40]:

$$\dot{Q}_{sh,b} = \rho_a V_{a,b}(T_{in}^{\lambda+1} - T_{in}^{\lambda}) + \rho_a \dot{V}_{ven}(T_{in} - T_{out}) + UA_{l,b}(T_{in} - T_{out}) + \rho_{bm} V_{bm}(T_{bm}^{\lambda+1} - T_{bm}^{\lambda}) - \sum_{n=1}^{M} A_n I_T (\tau\alpha)_{avg} \quad (27)$$

Where, T, V, ρ, $\dot{V}_{ven}$, $UA_{l,b}$, A_n, I_T, $(\tau\alpha)_{avg}$ and M are temperature, volume, density, Entering air for ventilation, building heat loss coefficient, area of each window, solar irradiation through windows, windows average transmission-absorption coefficient and the inside components of the structure visible to the sun rays and total number of spaces letting sun rays coming into the structure, respectively. The superscript λ is the time step counter, while the subscripts *in* /*out*, *b*, *bm* and *a* refer to the indoor / ambient condition, the building, the building stuck material and the air within the building, respectively. The first term in the right side of the equation is the required heat to increase the indoor temperature. The second and the third terms are the rates of heat losses due to the air ventilation and to the environment, respectively. Since the rate of energy storage in the building stuck is supposed to be zero under the steady state conditions, the fourth term is neglected. The last term indicates the rate of heat absorbed from the sun due to the solar irradiation.

The space cooling (SPC) demand can be obtained in the same way as that used for SPH demand.

The electricity grid considered for the network is a typical grid allowing for bidirectional power flows between the local facilities/buildings and the distribution network. It is assumed that power lines/cables are well sized; thus, they could carry the needed power without reaching thermal constraints. To obtain the electricity demand of the network, the in-building appliances and number of the residents within the houses should be specified. The nominal electricity consumptions of the electrical components of the buildings are listed as in Table 7 [41]. To make the results more generalized, different numbers of residents are considered (see Table 1).

Sepehr et al. [41] has described in detail the methodology of calculating the electrical load of buildings. Based on this methodology, using the equipment listed in Table 7 and the number of residents in each building outlined in Table 1, the electricity demand of the network can be estimated over a geographical area. In order to randomize the behavior of the consumers, a bottom-up approach is developed with a given resolution (e.g. one minute).

Table 7

The list of equipment in each house with the nominal power

Application	**Nominal power (kW)**	**Application**	**Nominal power (kW)**

Refrigerator	0.11	TV 1	0.105
Freezer	0.11	TV 2	0.083
Microwave oven	1.5	Computer / laptop	0.11
Coffee maker	1	Other occasional load	1
Range oven	1.05	Clothes washer	1.2
Hair dryer	1.6	Lighting	0.12

In the end, the rate of heat losses/gains, which is vital in thermodynamic modeling of DH/DC systems, should be calculated. The following correlation is used to obtain the thermal energy losses from twine-pipes of DH and DC systems [42]:

$$\dot{Q}_l = \frac{7.992}{T_R T_S^2 D_R^{0.5}} - \frac{374.1391}{T_S T_R^{1.5} D_R^2} + \frac{166.9072}{T_R D_R^{1.5}} + \frac{171.3874 T_S T_R}{D_R^2} + 0.28356 T_S^{1.5} T_R^{1.5} D_R^2 - 16.9348 \quad (28)$$

The details of how this correlation has been developed could be found in Ref. [42].

3.4. Exergy analysis and sustainability index

Exergy analysis is a powerful tool to find the exact value of the systems' irreversibility and losses during the thermodynamic processes [43]. As stated by Bejan et al., exergy can be defined in terms of four components: physical, kinetic, potential, and chemical exergy [44]. Kinetic and potential exergy was neglected in the present study and since variations in the compositions of flow streams did not occur, the chemical exergy was not considered [29]. For comprehensive introduction to the exergy principle, refer to the textbooks of Kotas [45], Moran et al. [46] or Szargut et al. [47].

In the present study, exergy rates associated with the geothermal source and waste heat source are considered as the fuel exergy for the geothermal-driven and waste heat-driven CCHPs, respectively. Accordingly, the exergy rates associated with the produced SPH, SPC, DHW and electricity are considered as the products exergy. Second law efficiency can be written as [48,49]:

$$\eta_{II} = \frac{\dot{E}_{product}}{\dot{E}_{fuel}} \quad (29)$$

On the other hand, exergy concept has a tight relation with the sustainable development and environmental impacts which can be described via a sustainability index [50]. Sustainable development is defined in different ways, but the most frequently used definition refers to "a development which meets the needs of the present without compromising the ability of future generations to meet their own needs" [51]. Sustainability index emphasizes the fact that not only sustainable and renewable energies should be developed and utilized more and more, but also the available non-renewable energy sources like natural gas or nuclear energy should be used in the most efficient way. In fact, sustainability index states how exergy destruction reduction can lead to decreasing the environmental impact and can be defined as [52–54]:

$$SI = \frac{1}{D_P} \tag{30}$$

here, D_P is the destroyed exergy divided by input exergy (a depletion number) [55,56]:

$$D_P = \frac{\dot{E}_D}{\dot{E}_{in}} \tag{31}$$

4. Results and discussion

Thermal energy and thermomechanical exergy contents of the industrial waste heat and geothermal energy were calculated to show the energy and exergy that can be harvested for the case study energy network. Table 8 lists the calculated values. In this table, the available energy/exergy refers to the difference between the energy/exergy of the energy source at its present conditions and at ambient temperature.

Table 8

Energy and exergy of the contents of the energy resources

Energy source	Cement factory waste heat	Geothermal
Available thermal energy (kW)	4409	6546
Available thermomechanical exergy (kW)	1133	707.8

Hereunder, the results of the simulations and analysis carried out on the considered DH and DC system including both CCHPs will be presented. In this regard, the thermodynamic performance of the considered CCHPs, and their production capacity of SPH and cooling, DHW and electricity will be reported initially. As mentioned before, flexibility of supplying different values of SPC was supposed in the CCHPs design due to the fact that heating and cooling demand varies during different seasons. It should be mentioned that in this section the average ambient temperature is considered to evaluate the exergy and sustainability performance of the CCHPs. Table 9 lists the systems' capacity under the base condition and the cost of products, which are obtained using exergoeconomic analysis [57]. On the other hand, for more general results, different values of cooling load are reported. It is clear that a change in the cooling capacity of the systems may alter the other products capacity. Table 10 outlines the range of SPH and cooling, DHW and electricity, which would be possible to be delivered to the network. As can be seen, the proposed local energy systems are designed in such a way that higher cooling production is favorable for the geothermal-driven CCHP from the thermodynamics and sustainability points of view while reducing cooling production improves the waste heat-driven CCHPs' performance.

Table 9

Supplied SPH, SPC, DHW and electricity by each CCHP under the base condition

Parameter	Geothermal-driven CCHP	Waste heat-driven CCHP	Total	Cost (€/MWh)
SPC (kW)	529.7	295.1	824.8	5.688
SPH (kW)	3018	2119	5137	11.811
Electricity(kW)	116.3	608.3	724.6	10.109
DHW (kW)	1744	594.2	2338.2	3.381
η_{II} (%)	49.63	63.6	-	-
SI (-)	1.985	2.747	-	-

Table 10

Range of supplied SPH, SPC, DHW and electricity by each CCHP

Parameter	Geothermal-driven CCHP	Waste heat-driven CCHP	Total
SPC (kW)	0 - 1049	0 - 590.2	0 – 1639.2
SPH (kW)	6035 - 0	2119	8154 - 2119
Electricity (kW)	232.6 – 0	608.3	840.9 – 608.3
DHW (kW)	0 - 3454	1188 - 0	1188 - 3454

η_{II} (%)	39.78 - 59.28	67.62 - 59.57	-
SI (-)	1.661 - 2.456	3.089 - 2.473	-

The two effective environmental parameters with remarkable effects on the DH and DC system are the ambient temperature and solar energy availability in the case study. Fig. 5 presents information regarding these parameters over the entire year. As can be seen from this figure, the ambient temperature can be low as around -1 °C which would increase the DH demand, while can be high as 35 °C during summertime clarifying the importance of the cooling network. Furthermore, sun radiation has a considerable effect on the SPC demand, especially in the summer days. As it is illustrated in detail in Fig. 6, during the sunny days solar radiation reaches to 1kW on a horizontal surface, while not much solar energy is expected during the cold days as the irradiation decreases to almost 0.37 kW. Jun 29 and Dec 24 are reported as the days with the highest and lowest solar radiation, respectively, for the case study.

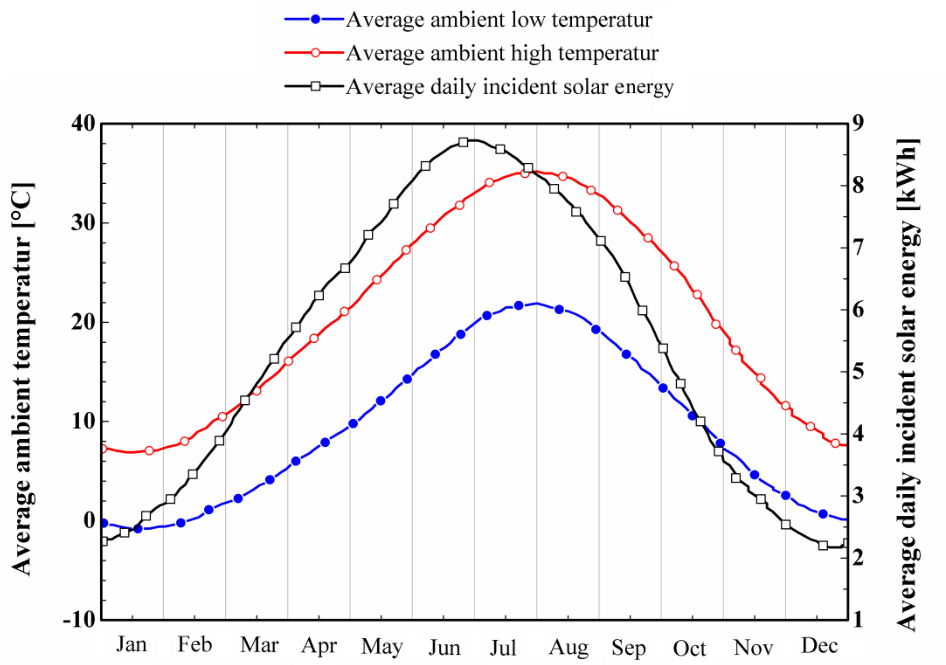

Fig. 5 Average ambient high and low temperature and average daily incident solar energy of the considered residential area in Gaziantep, Turkey over an entire year

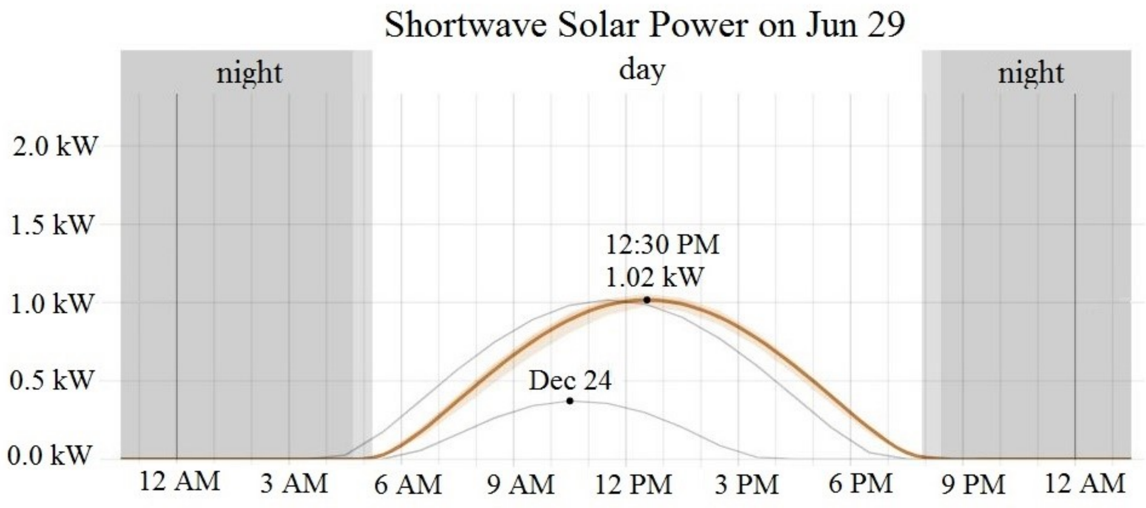

Fig. 6 Solar radiation in the considered residential area in Gaziantep, Turkey over Jun 29 and Dec 24

Before analyzing the consumers' consumption pattern and its interaction with the proposed CCHPs within the DH and DC network, we investigate the effects of the ambient temperature on the exergetic and sustainability performance of the CCHPs. Figs. 7 and 8 illustrate exergy efficiency and sustainability index of the geothermal- and waste heat-driven CCHPs, respectively, under the base condition. As it was expected, during summertime, exergy efficiency and sustainability index of the both systems decrease mainly due to a reduction in the exergy rate associated with the supplied DH. In fact, during the cold days, as the ambient temperature decreases, temperature difference between dead state (which is of importance from the exergy point of view) and delivered DH increases and results in DH higher exergy rates. During the entire year, exergy efficiency of the geothermal- and waste heat-driven CCHPs varies between 40.6-53.46% and 62.28-64.1%, respectively. Moreover, sustainability index of 1.586-2.148 and 2.651-2.785 are obtained for the geothermal- and waste heat-driven CCHPs, respectively.

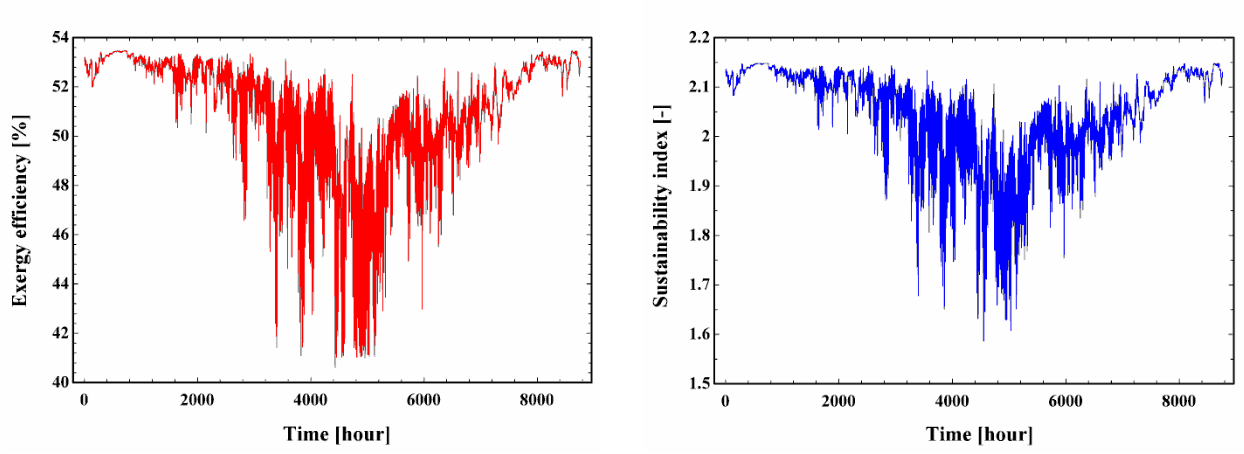

(a) (b)

Fig. 7 Exergetic and sustainability performance of the geothermal-driven CCHP with ambient temperature over the entire year

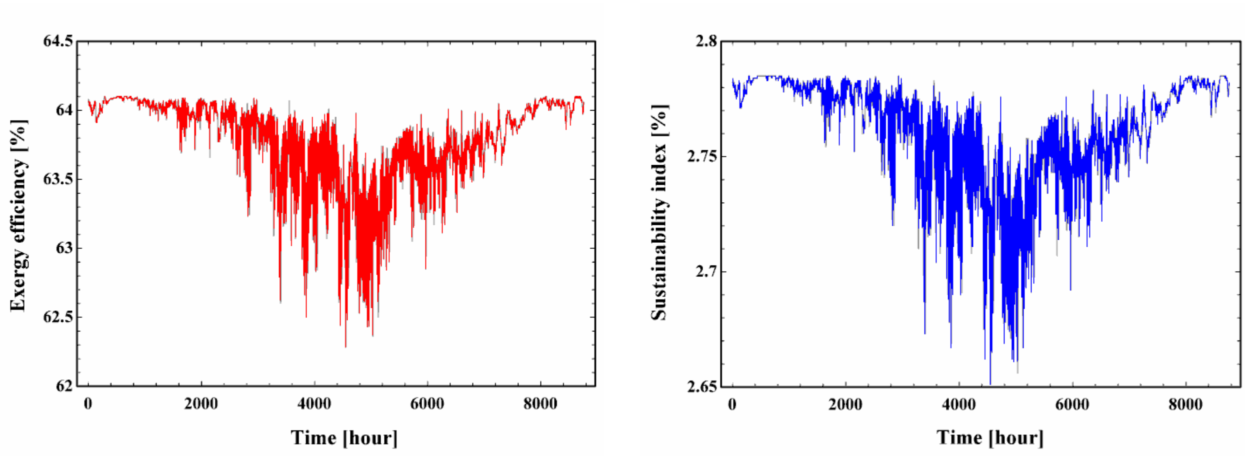

(a) (b)

Fig. 8 Exergetic and sustainability performance of the waste heat-driven CCHP with ambient temperature over the entire year

Fig. 9 illustrates total energy demand by the case study and overproduced energy by the considered local CCHPs, which can be transferred to the main grid. Fig. 9(a) presents the DHW draw-off pattern of a couple of randomly selected houses in the network and the overproduced hot water over a day (Fig. 9(b)), which can be transferred to the hot water grid. It is supposed that the daily pattern is repeated over the entire year. Then calculations are reported just for one day with a time granularity of one minute. As can be seen from Fig. 9(a), DHW consumption by the case study varies between 0 and 188 kW and this amount of demand can be completely fed by the proposed local energy system. In this way, an extra 2830-3018 kW hot water can be supplied to the main grid of DHW supply.

Fig. 9(c) indicates the electricity consumption profile by the subscribers in a typical day. Since no air conditioning is needed for the considered buildings and seasonal changes do not affect electricity consumption pattern considerably, then the demand profile will be repetitive during the entire year. Based on Fig. 9(d), the local energy system supplies the electricity demand and feeds the main grid by its surplus power most of the time. However, for the time span of 830-850 and 1330-1430 minutes (i.e., the peak period) the overall electricity consumption is beyond the capacity of the local system thus necessitates power import from the mains. The maximum electricity that is needed to be fed by the main grid is almost 387 kW. During the off-peak period, however, the local energy system is able to charge the main grid with a maximum electric power of 677.6 kW.

Since a range of indoor comfort temperature is considered for the winter days, there will be a lower and upper boundary for the required heat. Fig. 9(e) and (f) show the SPH demand by the case study and surplus heating produced by the local designed CCHPs as the SPH. Overproduced SPH can be injected to the main heating grid via pressurized medium-temperature water. As can be seen from the Fig. 9(e), the maximum heat demand changes between 717 and 861 kW within the first months of the year for the comfort temperature of 20 and 24 °C, respectively. It is clear that the lowest value of the required SPH belongs to the summer days. In this condition, designed local CCHPs not only supplies the required heat, but also provides more than 5100 kW extra heating to the main grid, as Fig. 9(f) represents.

Similarly, required cooling for the SPC is calculated for the entire year and it has lower and upper boundaries due to considering a range of comfort temperature. Fig. 9(g) indicates the obtained values of the SPC demand of the examined system, while the surplus cooling produced by the CCHPs is shown in Fig. 9(h). SPC demand touches the maximum value of 526.8 and 631 kW for the indoor comfort temperature of 27 and 24 °C, respectively. This high value of cooling demand is mainly due to the high ambient temperature and solar radiation for the summer days as illustrated in Fig. 5. Based on the obtained results, proposed local CCHPs have a surplus of 193.8 – 824.8 kW cooling energy, which can be delivered to the main grid.

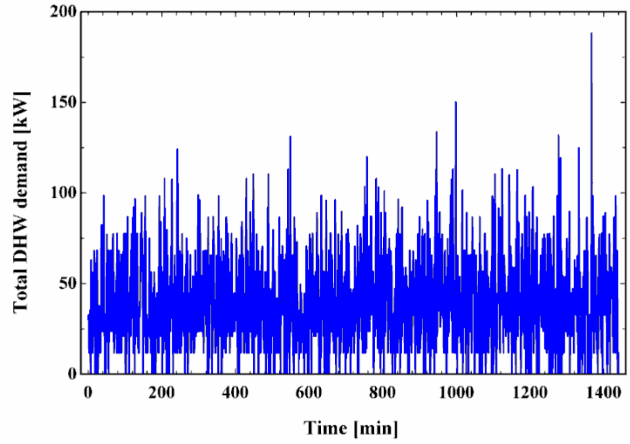
Total DHW demand [kW]
Time [min]

(a)

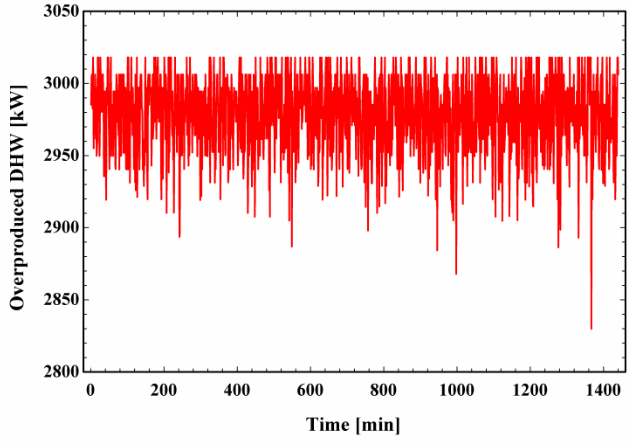
Overproduced DHW [kW]
Time [min]

(b)

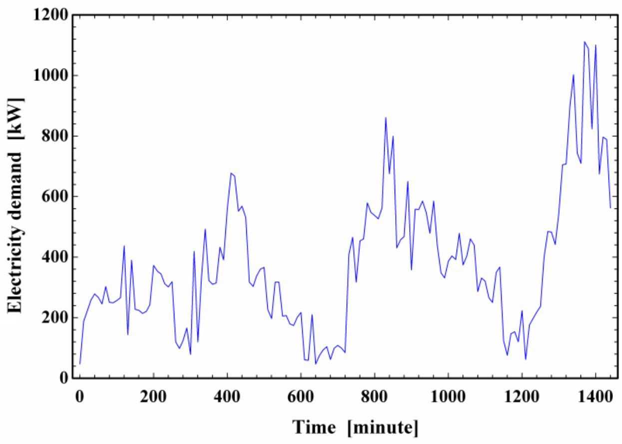
Electricity demand [kW]
Time [minute]

(c)

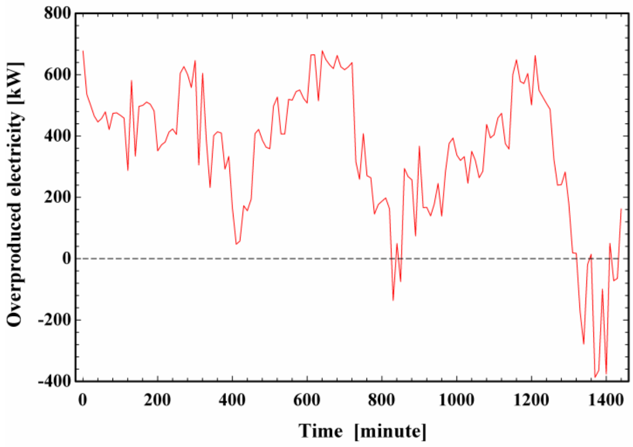
Overproduced electricity [kW]
Time [minute]

(d)

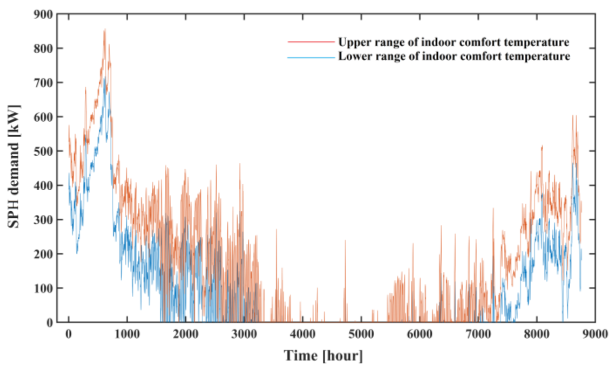
Upper range of indoor comfort temperature
Lower range of indoor comfort temperature
SPH demand [kW]
Time [hour]

(e)

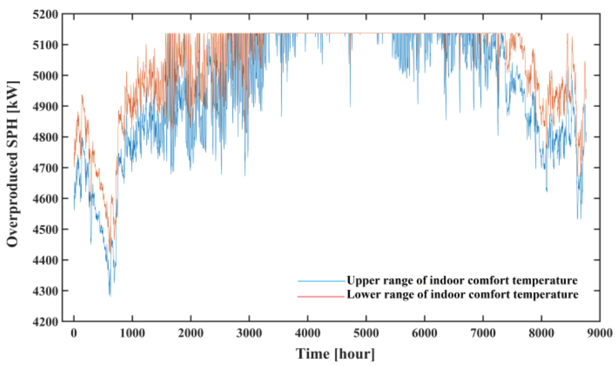
Upper range of indoor comfort temperature
Lower range of indoor comfort temperature
Overproduced SPH [kW]
Time [hour]

(f)

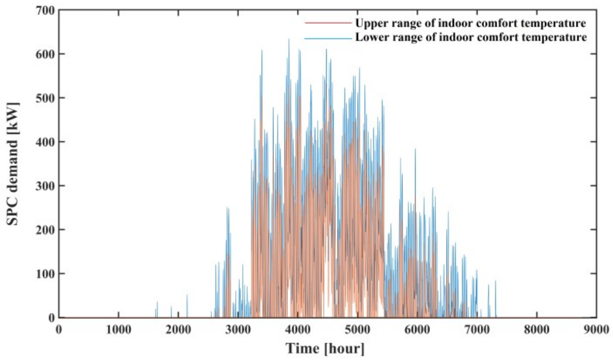

(g)

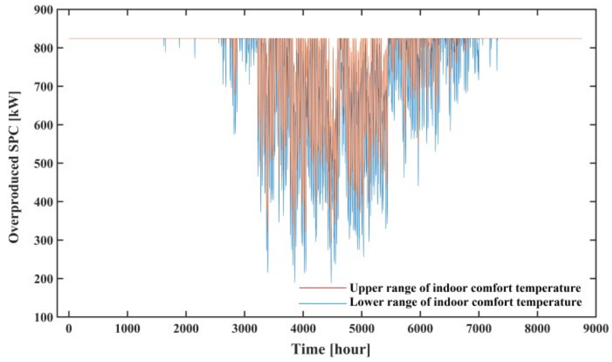

(h)

Fig. 9 Total demand of (a) DHW, (c) electricity, (e) SPH, (g) SPC of the examined system and overproduced (b) DHW, (d) electricity, (f) SPH, (h) SPC by the proposed CCHPs

As it is obtained, the local energy system based on geothermal and waste heat-driven CCHPs is able to supply the energy demand of the considered residential area in terms of DHW, SPH, SPC and electricity. In addition, most of the time, this local energy system produces surplus energy, which will be transferred to the main grid. However, in analyzing an energy conversion system, not only thermodynamic and sustainability should be considered, but also enough attention should be paid on the economic criteria. The latter is of a great significance from the end-users' perspective as the energy consumption cost can be substantially decreased through use of local energy systems instead of main grids. To further investigate the economic aspect, Table 11 shows simulation results regarding annual households' payment for their energy demand (as shown in Fig. 9) supplied by the main grid and the designed local energy systems. In these calculations, it is assumed that cost of the electricity supplied by the main grid is 20 €/MWh [58], while cost of heating and cooling is almost 15 €/MWh. Cost of energy provision by the local energy system is also listed in Table 8. As proved by Table 11, the highest payment belongs to the SPH, while the highest economic benefit refers to the SPC. This is because the unit cost of SPC supplied by the designed energy system is much lower than that the one by the main grid. Considering all types of energy demand in the case study, almost 15687 € will be saved for the households with employing the proposed local energy system.

Table 11

Households' payment for their energy demand supplied by the main grid and the designed local energy system

Different forms of energy	SPH	SPC	DHW	Electricity	Total
Cost of energy supplied via the main grid (€/year)	18168	7315	5206	6569	37258

Cost of energy supplied via designed local CCHPs (€/year)	14304	2774	1173	3320	21571
Economic benefits of households (€/year)	3864	4541	4033	3249	15687

5. Conclusions and Recommendation

Energy systems are moving towards integrated designs for supplying electricity, space conditioning and DHW via power, heat and cold distribution grids. Distributed energy systems are promising due to reducing the production and transportation costs and enabling to use free/cheap low quality energy sources (e.g. low- and medium-temperature geothermal, waste heat from different industries, etc.). Utilizing low quality energy sources is such important that has been addressed as one of the 17 sustainable development goals of the UN.

This study investigated the use of waste heat and low-medium temperature geothermal heat sources to run small-scale CCHPs for domestic heating, cooling and electricity applications in a case study in Turkey. A residential neighborhood was considered as the case study in which the energy demands of buildings (electricity, hot water and space conditioning) were mainly supposed to be supplied by the designed CCHPs. The CCHPs are equipped with ORC, single effect LiBr-H2O absorption chiller and auxiliary heat exchangers. Both supply- and demand-side were analyzed in detail using energy and exergy principles to dig into deep thermodynamic time-dependent performance of the network. Then, energy demand of the buildings in the case study was determined over an entire year. The main conclusions out of the thermodynamic and economic simulations of the CCHPs are as:

- Under the base condition, exergy efficiency / sustainability index of 49.63 % / 1.985 and 63.6 % / 2.747 were obtained for the geothermal and waste heat-driven CCHP, respectively.
- The designed energy system was able not only to feed the whole energy demand of the case study, but also to provide a considerable value of surplus energy to the main grid.
- In terms of payment value by the end user consumers for their energy demand, the proposed system could bring a significant benefit. Since the supplied energy by the proposed system has lower cost compared to that of the main grid, it was possible to save around 15687 € per year for the case study.

In addition, the following subjects are suggested for future extension of this work:

- Employing different kinds of renewable energy sources and comparing the thermodynamic and economic results with those reported in the present study.

- Exergoeconomic and exergoenvironmental analyses of the presented system using the emergy concept as developed by Aghbashlo et al. [59].
- Environmental analysis of the proposed energy network and comparing the findings with the existing conventional energy systems.

Acknowledgment

This research is part of the "*HeatReFlex-Green and Flexible District Heating/Cooling*" project (www.heatreflex.et.aau.dk) funded by Danida Fellowship Centre and the Ministry of Foreign Affairs of Denmark to conduct research in growth and transition countries under the grant no. 18-M06-AAU.

Nomenclature

Abbreviations

CCHP	combined heating, cooling and power
Cond	condenser
DC	district cooling
DH	district heating
DHW	domestic hot water
Gen	generator
HE	heat exchanger
HW	hot water
IHE	internal heat exchanger
ORC	organic Rankine cycle
ORCC	ORC unit condenser
ORCE	ORC unit evaporator
ORCP	ORC unit pump
ORCT	ORC unit turbine
P	pump
SHE	solution heat exchanger
SPC	space cooling
SPH	space heating

Latin letters

e	specific physical exergy (kJ/kg)
eff	effectiveness
$\dot{E}$	exergy flow rate (kW)
h	specific enthalpy (J/kg)
$\dot{m}$	mass flow rate (kg/s)
$\dot{Q}$	heat transfer rate (kW)
s	entropy (kJ/kg K)
T	temperature (K)
V	volume
$\dot{W}$	power (kW)

Greek letters

η	energy efficiency (-)
η_{II}	exergy efficiency (-)
η_{is}	isentropic efficiency
ρ	density
ε	exergy efficiency (-)

Subscripts

ch	chemical
cv	control volume
D	destruction
e	outlet
i	inlet
o	outlet
ph	physical
ven	ventilation
0	ambient conditions

References

[1] I. Dincer, C. Acar, Smart energy systems for a sustainable future, Appl. Energy. 194 (2017) 225–235. https://doi.org/10.1016/J.APENERGY.2016.12.058.

[2] H. Lund, N. Duic, P.A. Østergaard, B.V. Mathiesen, Smart energy systems and 4th generation district heating, Energy. 110 (2016) 1–4. https://doi.org/10.1016/j.energy.2016.07.105.

[3] A. Arabkoohsar, Non-uniform temperature district heating system with decentralized heat pumps and standalone storage tanks, Energy. 170 (2019) 931–941. https://doi.org/10.1016/J.ENERGY.2018.12.209.

[4] B.V. Mathiesen, H. Lund, D. Connolly, H. Wenzel, P.A. Østergaard, B. Möller, S. Nielsen, I. Ridjan, P. Karnøe, K. Sperling, F.K. Hvelplund, Smart Energy Systems for coherent 100% renewable energy and transport solutions, Appl. Energy. 145 (2015) 139–154. https://doi.org/10.1016/J.APENERGY.2015.01.075.

[5] S. Buffa, M. Cozzini, M. D'Antoni, M. Baratieri, R. Fedrizzi, 5th generation district heating and cooling systems: A review of existing cases in Europe, Renew. Sustain. Energy Rev. 104 (2019) 504–522. https://doi.org/10.1016/J.RSER.2018.12.059.

[6] B. Rezaie, M.A. Rosen, District heating and cooling: Review of technology and potential enhancements, Appl. Energy. 93 (2012) 2–10. https://doi.org/10.1016/J.APENERGY.2011.04.020.

[7] H. Lund, S. Werner, R. Wiltshire, S. Svendsen, J.E. Thorsen, F. Hvelplund, B.V. Mathiesen, 4th Generation District Heating (4GDH): Integrating smart thermal grids into future sustainable energy

systems, Energy. 68 (2014) 1–11. https://doi.org/10.1016/J.ENERGY.2014.02.089.

[8] A. Inayat, M. Raza, District cooling system via renewable energy sources: A review, Renew. Sustain. Energy Rev. 107 (2019) 360–373. https://doi.org/10.1016/J.RSER.2019.03.023.

[9] O. Todorov, K. Alanne, M. Virtanen, R. Kosonen, A method and analysis of aquifer thermal energy storage (ATES) system for district heating and cooling: A case study in Finland, Sustain. Cities Soc. 53 (2020) 101977. https://doi.org/10.1016/j.scs.2019.101977.

[10] S. Chen, X. Zhang, S. Wei, T. Yang, J. Guan, W. Yang, L. Qu, Y. Xu, An energy planning oriented method for analyzing spatial-temporal characteristics of electric loads for heating/cooling in district buildings with a case study of one university campus, Sustain. Cities Soc. 51 (2019) 101629. https://doi.org/10.1016/j.scs.2019.101629.

[11] K. Saberi, H. Pashaei-Didani, R. Nourollahi, K. Zare, S. Nojavan, Optimal performance of CCHP based microgrid considering environmental issue in the presence of real time demand response, Sustain. Cities Soc. 45 (2019) 596–606. https://doi.org/10.1016/j.scs.2018.12.023.

[12] E. Oró, P. Taddeo, J. Salom, Waste heat recovery from urban air cooled data centres to increase energy efficiency of district heating networks, Sustain. Cities Soc. 45 (2019) 522–542. https://doi.org/10.1016/j.scs.2018.12.012.

[13] A. Peltokorpi, M. Talmar, K. Castrén, J. Holmström, Designing an organizational system for economically sustainable demand-side management in district heating and cooling, J. Clean. Prod. 219 (2019) 433–442. https://doi.org/10.1016/J.JCLEPRO.2019.02.106.

[14] A. Hepbasli, Low exergy (LowEx) heating and cooling systems for sustainable buildings and societies, Renew. Sustain. Energy Rev. 16 (2012) 73–104. https://doi.org/10.1016/J.RSER.2011.07.138.

[15] H. Dorotić, T. Pukšec, N. Duić, Multi-objective optimization of district heating and cooling systems for a one-year time horizon, Energy. 169 (2019) 319–328. https://doi.org/10.1016/J.ENERGY.2018.11.149.

[16] T. Sommer, S. Mennel, M. Sulzer, Lowering the pressure in district heating and cooling networks by alternating the connection of the expansion vessel, Energy. 172 (2019) 991–996. https://doi.org/10.1016/J.ENERGY.2019.02.010.

[17] J. von Rhein, G.P. Henze, N. Long, Y. Fu, Development of a topology analysis tool for fifth-generation district heating and cooling networks, Energy Convers. Manag. 196 (2019) 705–716. https://doi.org/10.1016/J.ENCONMAN.2019.05.066.

[18] E. Popovski, T. Fleiter, H. Santos, V. Leal, E.O. Fernandes, Technical and economic feasibility of

sustainable heating and cooling supply options in southern European municipalities-A case study for Matosinhos, Portugal, Energy. 153 (2018) 311–323. https://doi.org/10.1016/J.ENERGY.2018.04.036.

[19] N. Kabalina, M. Costa, W. Yang, A. Martin, Impact of a reduction in heating, cooling and electricity loads on the performance of a polygeneration district heating and cooling system based on waste gasification, Energy. 151 (2018) 594–604. https://doi.org/10.1016/J.ENERGY.2018.03.078.

[20] A. Carotenuto, R.D. Figaj, L. Vanoli, A novel solar-geothermal district heating, cooling and domestic hot water system: Dynamic simulation and energy-economic analysis, Energy. 141 (2017) 2652–2669. https://doi.org/10.1016/J.ENERGY.2017.08.084.

[21] M. Yari, Exergetic analysis of various types of geothermal power plants, Renew. Energy. 35 (2010) 112–121. https://doi.org/10.1016/j.renene.2009.07.023.

[22] A.F. Altun, M. Kilic, Thermodynamic performance evaluation of a geothermal ORC power plant, Renew. Energy. 148 (2020) 261–274. https://doi.org/10.1016/j.renene.2019.12.034.

[23] A. Moallemi, A. Arabkoohsar, F.J.P. Pujatti, R.M. Valle, K.A.R. Ismail, Non-uniform temperature district heating system with decentralized heat storage units, a reliable solution for heat supply, Energy. (2018). https://doi.org/https://doi.org/10.1016/j.energy.2018.10.188.

[24] F. Mohammadkhani, N. Shokati, S.M.S. Mahmoudi, M. Yari, M.A. Rosen, Exergoeconomic assessment and parametric study of a Gas Turbine-Modular Helium Reactor combined with two Organic Rankine Cycles, Energy. 65 (2014) 533–543.

[25] M. Yari, Performance analysis of the different Organic Rankine Cycles (ORCs) using dry fluids, Int. J. Exergy. 6 (2009) 323. https://doi.org/10.1504/IJEX.2009.515621.

[26] H.D. Madhawa Hettiarachchi, M. Golubovic, W.M. Worek, Y. Ikegami, Optimum design criteria for an Organic Rankine cycle using low-temperature geothermal heat sources, Energy. 32 (2007) 1698–1706. https://doi.org/10.1016/j.energy.2007.01.005.

[27] S.M. Alirahmi, S. Rahmani Dabbagh, P. Ahmadi, S. Wongwises, Multi-objective design optimization of a multi-generation energy system based on geothermal and solar energy, Energy Convers. Manag. 205 (2020) 112426. https://doi.org/10.1016/j.enconman.2019.112426.

[28] A. Hepbasli, C. Canakci, Geothermal district heating applications in Turkey: a case study of Izmir–Balcova, Energy Convers. Manag. 44 (2003) 1285–1301. https://doi.org/10.1016/S0196-8904(02)00121-8.

[29] H. Nami, I.S. Ertesvåg, R. Agromayor, L. Riboldi, L.O. Nord, Gas turbine exhaust gas heat recovery by organic Rankine cycles (ORC) for offshore combined heat and power applications - Energy and exergy analysis, Energy. 165 (2018) 1060–1071. https://doi.org/10.1016/j.energy.2018.10.034.

[30] H. Nami, A. Arabkoohsar, A. Anvari-Moghaddam, Thermodynamic and sustainability analysis of a municipal waste-driven combined cooling, heating and power (CCHP) plant, Energy Convers. Manag. 201 (2019). https://doi.org/10.1016/j.enconman.2019.112158.

[31] A.A. H. Nami, Improving the Power Share of Waste-Driven CHP Plants via Parallelization with a Small-Scale Rankine Cycle, a Thermodynamic Analysis, Energy. In Press (2019).

[32] A. Arabkoohsar, Non-uniform temperature district heating system with decentralized heat pumps and standalone storage tanks, Energy. 170 (2019) 931–941. https://doi.org/10.1016/J.ENERGY.2018.12.209.

[33] A. Arabkoohsar, G.B. Andresen, Supporting district heating and cooling networks with a bifunctional solar assisted absorption chiller, Energy Convers. Manag. 148 (2017) 184–196. https://doi.org/10.1016/J.ENCONMAN.2017.06.004.

[34] E. Akrami, A. Chitsaz, H. Nami, S.M.S. Mahmoudi, Energetic and exergoeconomic assessment of a multi-generation energy system based on indirect use of geothermal energy, Energy. 124 (2017). https://doi.org/10.1016/j.energy.2017.02.006.

[35] A. Bejan, Advanced engineering thermodynamics, John Wiley & Sons, 2016.

[36] A. Razmi, M. Soltani, C. Aghanajafi, M. Torabi, Thermodynamic and economic investigation of a novel integration of the absorption-recompression refrigeration system with compressed air energy storage (CAES), Energy Convers. Manag. 187 (2019) 262–273. https://doi.org/10.1016/j.enconman.2019.03.010.

[37] A. Atmaca, R. Yumrutaş, Thermodynamic and exergoeconomic analysis of a cement plant: Part II – Application, Energy Convers. Manag. 79 (2014) 799–808. https://doi.org/10.1016/J.ENCONMAN.2013.11.054.

[38] A. Razmi, M. Soltani, M. Tayefeh, M. Torabi, M.B. Dusseault, Thermodynamic analysis of compressed air energy storage (CAES) hybridized with a multi-effect desalination (MED) system, Energy Convers. Manag. 199 (2019). https://doi.org/10.1016/j.enconman.2019.112047.

[39] A. Anvari-Moghaddam, H. Monsef, A. Rahimi-Kian, Cost-effective and comfort-aware residential energy management under different pricing schemes and weather conditions, Energy Build. 86 (2015) 782–793. https://doi.org/10.1016/J.ENBUILD.2014.10.017.

[40] A. Anvari-Moghaddam, H. Monsef, A. Rahimi-Kian, Optimal Smart Home Energy Management Considering Energy Saving and a Comfortable Lifestyle, IEEE Trans. Smart Grid. 6 (2015) 324–332. https://doi.org/10.1109/TSG.2014.2349352.

[41] M. Sepehr, R. Eghtedaei, A. Toolabimoghadam, Y. Noorollahi, M. Mohammadi, Modeling the

electrical energy consumption profile for residential buildings in Iran, Sustain. Cities Soc. 41 (2018) 481–489. https://doi.org/10.1016/J.SCS.2018.05.041.

[42] A.S. Alsagri, A. Arabkoohsar, M. Khosravi, A.A. Alrobaian, Efficient and cost-effective district heating system with decentralized heat storage units, and triple-pipes, Energy. 188 (2019) 116035. https://doi.org/10.1016/j.energy.2019.116035.

[43] A.R. Razmi, M. Janbaz, Exergoeconomic assessment with reliability consideration of a green cogeneration system based on compressed air energy storage (CAES), Energy Convers. Manag. 204 (2020). https://doi.org/10.1016/j.enconman.2019.112320.

[44] F. Mohammadkhani, M. Yari, F. Ranjbar, A zero-dimensional model for simulation of a Diesel engine and exergoeconomic analysis of waste heat recovery from its exhaust and coolant employing a high-temperature Kalina cycle, Energy Convers. Manag. 198 (2019) 111782. https://doi.org/10.1016/J.ENCONMAN.2019.111782.

[45] T.J. Kotas, The exergy method of thermal plant analysis, 1st ed., Butterworths, London, 1998.

[46] M.J. Moran, H.N. Shapiro, D.D. Boettner, M.B. Bailey, Principles of engineering thermodynamics, eighth ed, John Wiley & Sons, 2015.

[47] J. Szargut, D.R. Morris, F.R. Steward, Exergy analysis of thermal, chemical, and metallurgical processes, Hemisphere, Philadelphia., USA, 1988.

[48] A. Razmi, M. Soltani, F. M. Kashkooli, L. Garousi Farshi, Energy and exergy analysis of an environmentally-friendly hybrid absorption/recompression refrigeration system, Energy Convers. Manag. 164 (2018) 59–69. https://doi.org/10.1016/j.enconman.2018.02.084.

[49] A. Razmi, M. Soltani, M. Torabi, Investigation of an efficient and environmentally-friendly CCHP system based on CAES, ORC and compression-absorption refrigeration cycle: Energy and exergy analysis, Energy Convers. Manag. 195 (2019) 1199–1211. https://doi.org/10.1016/j.enconman.2019.05.065.

[50] I. Dincer, A.S. Joshi, Solar based hydrogen production systems, Springer, 2013.

[51] H. Nami, A. Anvari-Moghaddam, Small-scale CCHP systems for waste heat recovery from cement plants: Thermodynamic, sustainability and economic implications, Energy. (2020) 116634. https://doi.org/10.1016/J.ENERGY.2019.116634.

[52] P. Ahmadi, M.A. Rosen, I. Dincer, Multi-objective exergy-based optimization of a polygeneration energy system using an evolutionary algorithm, Energy. 46 (2012) 21–31. https://doi.org/10.1016/J.ENERGY.2012.02.005.

[53] P. Ahmadi, I. Dincer, M.A. Rosen, Exergo-environmental analysis of an integrated organic Rankine cycle for trigeneration, Energy Convers. Manag. 64 (2012) 447–453. https://doi.org/10.1016/J.ENCONMAN.2012.06.001.

[54] I. Dincer, M.M. Hussain, I. Al-Zaharnah, Energy and exergy use in the industrial sector of Saudi Arabia, Proc. Inst. Mech. Eng. Part A J. Power Energy. 217 (2003) 481–492. https://doi.org/10.1243/095765003322407539.

[55] A. Arabkoohsar, H. Nami, Thermodynamic and economic analyses of a hybrid waste-driven CHP–ORC plant with exhaust heat recovery, Energy Convers. Manag. 187 (2019) 512–522. https://doi.org/10.1016/j.enconman.2019.03.027.

[56] H. Nami, F. Ranjbar, M. Yari, Thermodynamic assessment of zero-emission power, hydrogen and methanol production using captured CO 2 from S-Graz oxy-fuel cycle and renewable hydrogen, Energy Convers. Manag. 161 (2018) 53–65.

[57] G. Tsatsaronis, L. Lin, J. Pisa, Exergy Costing in Exergoeconomics, J. Energy Resour. Technol. 115 (1993) 9. https://doi.org/10.1115/1.2905974.

[58] A. Arabkoohsar, M. Dremark-Larsen, R. Lorentzen, G.B. Andresen, Subcooled compressed air energy storage system for coproduction of heat, cooling and electricity, Appl. Energy. 205 (2017) 602–614. https://doi.org/10.1016/J.APENERGY.2017.08.006.

[59] M. Aghbashlo, M.A. Rosen, Consolidating exergoeconomic and exergoenvironmental analyses using the emergy concept for better understanding energy conversion systems, J. Clean. Prod. 172 (2018) 696–708. https://doi.org/10.1016/J.JCLEPRO.2017.10.205.